Buletin Profesi Insinyur 8(2) (2025) 079–083
http://dx.doi.org/10.20527/bpi.v8i2.301
ISSN 2654-5926

Forensic Study of Post-Fire Structural Beam Damage Using the Finite Element Method

Ahmad Najib Hidayatullah[1] Nursiah Chairunnisa[1]

[1] Master of Civil Engineering Study Program, Lambung Mangkurat University

✉ 2420828310007@mhs.ulm.ac.id

This study evaluates the accuracy of the finite element method (FEM) as a tool for post-fire forensic assessment of reinforced concrete members. Numerical simulations were conducted to model reinforced concrete beam specimens after fire exposure, using data from a previous experimental study. The analysis focused on comparing experimental and numerical load–deflection responses. The simulation results showed good agreement with the experimental behavior. The error in deflection at the maximum-load point was 0.009% for beam A0 and 1.02% for beam A7. Compared with A0, the fire-exposed beam (A7) exhibited a 5.08% reduction in load-carrying capacity and an 18.58% decrease in maximum deflection. Overall, the findings confirm that FEM can effectively support forensic evaluation of fire-induced damage in reinforced concrete beams.

Keywords: finite element method; post-fire assessment; reinforced concrete beam; ANSYS

Submitted: November 26, 2025
Revised: December 1, 2025
Accepted: December 18, 2025
Published: December 20, 2025

Introduction

Fire is one of the most significant hazards that can threaten the integrity and safety of structures (Kodur et al., 2025). Concrete is generally recognized for its relatively good fire resistance and is therefore often preferred for fire-resistant construction compared with structural steel members. However, during fire events, structural elements are inevitably subjected to severe thermal and mechanical effects. One advantage of concrete is its low thermal conductivity and high specific heat, which slow the rise of temperature within the inner layers of the material (Abdulrahman & Kadir, 2022). Nonetheless, fire can substantially degrade the mechanical properties of both concrete and steel reinforcement, thereby reducing the residual performance of reinforced concrete elements (Song et al., 2020). Elevated temperatures may induce microcracking due to thermal expansion, surface spalling, and discoloration of concrete. The associated loss of strength results from several mechanisms, including progressive chemical decomposition during heating and subsequent cooling. In addition, heat exposure reduces the bond between concrete and steel reinforcement, which further decreases load-bearing capacity (Suryanita et al., 2019).

In practice, post-fire structural assessment often relies on visual inspection supported by basic non-destructive testing (NDT) methods such as hammer tapping and ultrasonic pulse velocity testing. However, these techniques are limited because they primarily provide surface-level information and may involve considerable uncertainty, particularly when assessing internal damage in critical elements such as beams.

To address these limitations, finite element method (FEM)–based numerical modeling has become a powerful tool for post-fire structural analysis (Simwanda et al., 2023). This approach enables sequential thermo-mechanical analysis, starting with heat-transfer analysis to determine the temperature distribution across the beam cross-section, followed by structural analysis to evaluate changes in material properties, stress distribution, and residual capacity. High temperatures can significantly degrade the mechanical properties of both concrete and reinforcing steel (Kodur et al., 2025). Previous studies have also indicated that localized fire damage may be inferred from changes in sensitive structural responses, such as shifts in the neutral axis position, which can be simulated accurately using FEM (Reynders et al., 2025).

Accordingly, this study aims to conduct a forensic investigation of post-fire damage in reinforced concrete beams using the finite element method. Numerical modeling is performed using ANSYS 2025 R2 (Academic/Student version) to simulate beam behavior under fire exposure, validate damage patterns, and quantify discrepancies between experimental observations and numerical predictions.

Method

The research procedure aimed to validate the numerical model by reproducing the A0 and A7 beam specimens reported in a previous study (Abdulrahman & Kadir, 2022). The numerical results were then compared with the experimental observations in terms of crack patterns, load–deflection responses, and the

How to cite this article:
Hidayatullah A.N., Chairunnisa N. (2025). Forensic Study of Post-Fire Structural Beam Damage Using the Finite Element Method. *Buletin Profesi Insinyur*, 8(2), 79–83.

 ISSN 2654-5926

discrepancies between experimental and numerical outcomes.

Specimens and material properties

Two reinforced concrete beam types were considered: A0 and A7. Specimen A0 represented the control beam without exposure to elevated temperature, whereas specimen A7 was subjected to high-temperature exposure for 45 minutes prior to mechanical testing. Both specimens shared the same geometry and reinforcement layout. The concrete compressive strength at 28 days was 89 MPa, and the mechanical properties of reinforcing steel adopted from Abdulrahman and Kadir (2022) are summarized in Table 1.

Table 1 Mechanical properties of reinforcing steel (Abdulrahman & Kadir, 2022)

Bar Size	Diameter (mm)	Fy (MPa)	Fu (MPa)
12	11.76	536	648
10	9.76	581	717

All beams had identical dimensions, with a length of 2000 mm, a height of 250 mm, and a width of 200 mm. Longitudinal reinforcement consisted of three 12-mm bars in tension and two 10-mm bars in compression. Shear reinforcement was provided by 10-mm stirrups spaced at 150 mm along the beam. The reinforcement configuration is shown in Figures 1 and 2.

Thermal exposure input for A7

For the A7 specimen, thermal exposure was modeled for 45 minutes before structural loading. In Abdulrahman and Kadir (2022), furnace temperatures were recorded at 5-minute intervals, reaching 876 °C at 45 minutes. In this study, the reported furnace temperature history was used as the reference thermal boundary condition. For implementation in the numerical model, the thermal loading was applied as a transient heating scenario consistent with the reported exposure duration.

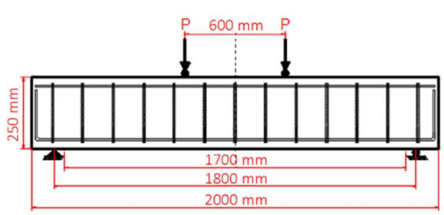

Figure 1 Test setup for the reinforced concrete beam (Abdulrahman & Kadir, 2022)

Finite element modeling in ANSYS

Finite element simulations were performed in ANSYS following three standard stages: pre-processing, solution, and post-processing. In the structural analysis, concrete was modeled using SOLID65 elements (ANSYS, 2025), which support nonlinear behavior and can represent tensile cracking and compressive crushing in reinforced concrete (Cottrell et al., 2021). Reinforcing bars were modeled using LINK180 elements (ANSYS, 2025), which effectively capture the axial tension–compression response of reinforcement (Krasnitskyi & Lobodanov, 2024).

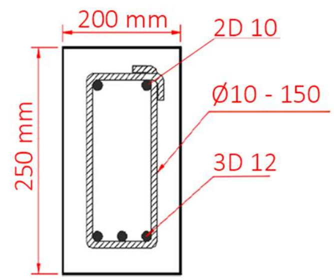

Figure 2 Cross-sections of the reinforced concrete beams (Abdulrahman & Kadir, 2022).

For beams exposed to elevated temperatures, a sequentially coupled thermo-mechanical approach was adopted. First, a transient thermal analysis was conducted to obtain the temperature distribution within the beam cross-section. Concrete was modeled using SOLID95 thermal elements (ANSYS, 2025), while reinforcement heat transfer was represented using LINK33 two-node thermal elements (Kumar & Kodur, 2023). The thermal analysis considered temperature-dependent heat transfer properties, including density, specific heat, and thermal conductivity. The resulting temperature field was then transferred to the structural model to evaluate the post-fire mechanical response.

For the structural response, concrete nonlinearity was represented using an appropriate nonlinear constitutive formulation available in ANSYS for reinforced concrete, while reinforcement was modeled as elastoplastic with isotropic hardening (ANSYS, 2025).

Results and Discussion

Load and deflection

The maximum load that a structural element can bear is referred to as the ultimate load (Pu). Beyond the ultimate load, damage to the structural element may occur. To determine ductility parameters, information on deformation at the ultimate load and corresponding deflection is required. Deformation can be evaluated through the load–deflection (δ) relationship curve. In this study, the highest deflection value obtained from numerical analysis was compared with the closest experimental deflection value, and the corresponding load values were then compared to determine the error difference.

The test data of concrete beam models A0 and A7 illustrate a comparison between experimental results and numerical analysis in terms of load and corresponding deflection values. Beam A0 served as the

Buletin Profesi Insinyur 8(2) (2025) 079–083 ISSN 2654-5926
http://dx.doi.org/10.20527/bpi.v8i2.301

control specimen and was not exposed to extreme temperatures, whereas beam A7 was exposed to extreme temperatures for 45 minutes. Experimental results for beam A0 showed a load of 118 kN with a deflection of 14.74 mm, while numerical analysis yielded a load of 125 kN with a deflection of 14.70 mm. For beam A7, the experimental results indicated a load of 112 kN with a deflection of 12.00 mm, whereas numerical analysis produced a load of 121.6 kN with a deflection of 11.88 mm. The load–deflection relationship of the concrete beams is presented in Figure 3.

Reinforced Concrete Beam Error Difference

Table 2 shows a high level of agreement between experimental and numerical analyses in predicting deflection at the maximum load point. For beam A0, the deflection difference was 0.009%, while for beam A7 it was 1.02%. With this consistency in deflection values, the numerical analysis using ANSYS is able to accurately represent the initial stiffness and deformation behavior of both reinforced concrete beams to a certain extent. These results indicate that the material parameters and boundary conditions applied in the ANSYS model are valid at the evaluated load levels.

In addition, the numerical model predicted higher maximum loads, with an increase of 5.95% for beam A0 and 8.57% for beam A7 compared to experimental results. According to Çalışkan et al. (2025), numerical simulations generally show a strong correlation with experimental tests, although minor differences may still occur due to material imperfections and boundary conditions that differ from real structural behavior.

The differences between experimental and numerical results for deflection and load are primarily caused by the sensitivity of ultimate load to constitutive material assumptions and boundary conditions. Deflection behavior is more strongly influenced by the global stiffness of the structure, which is generally well captured by numerical models. In contrast, ultimate load capacity is highly affected by local cracking behavior, concrete plasticity, and material imperfections that are difficult to model precisely using finite element analysis. Differences of up to ±10% between numerical and experimental results are generally considered acceptable for reinforced concrete capacity analysis (Luu et al., 2023; Çalışkan et al., 2025). Therefore, the differences observed in this study are considered valid for predicting the ultimate capacity of the beam specimens.

Cracking Patterns and Strength Drops

Figure 4 presents crack patterns that reflect changes in the physical properties of the material. Exposure to extreme temperatures can cause internal degradation of concrete, including the loss of bonded water, decomposition of cement paste, and the development of thermal microcracks, which collectively reduce concrete strength. As shown in Table 2, beam A7 experienced a reduction in load capacity of 5.08% (from 118 kN to 112 kN) and a reduction in maximum deflection of 18.58% (from 14.74 mm to 12.00 mm) compared to beam A0.

According to Antonius et al. (2019), experimental studies on reinforced concrete beams after fire exposure demonstrated significant reductions in ductility and deformation capacity, particularly in beams without double compression reinforcement. The numerical crack patterns in this study showed good agreement with experimental observations, characterized by dominant flexural cracks at midspan and reduced crack density in beam A7 after fire exposure. This behavior indicates degradation of tensile capacity due to high-temperature exposure.

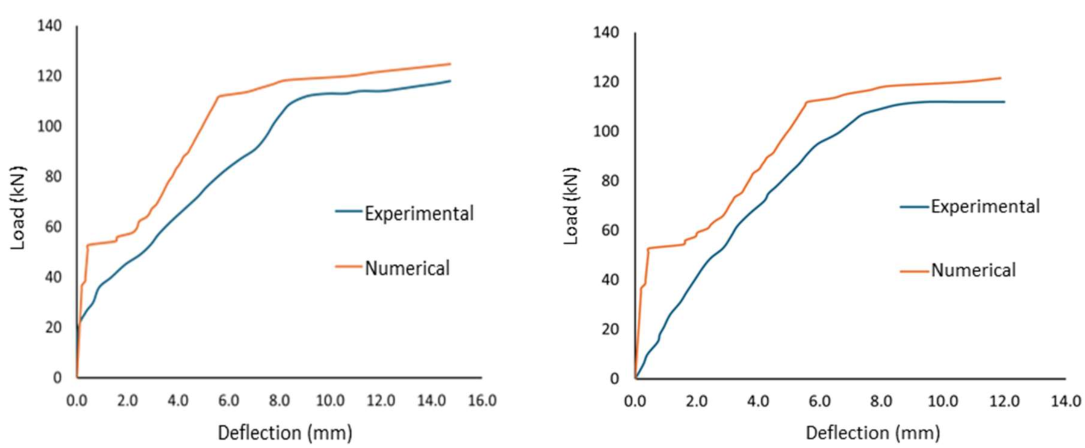

a) Beam load curve A0 **b)** A7 beam deflection load curve

Figure 3 Comparison of load–deflection curves from the experimental test and finite element analysis for A0 and A7 specimens.

Buletin Profesi Insinyur 8(2) (2025) 079–083
http://dx.doi.org/10.20527/bpi.v8i2.301 ISSN 2654-5926

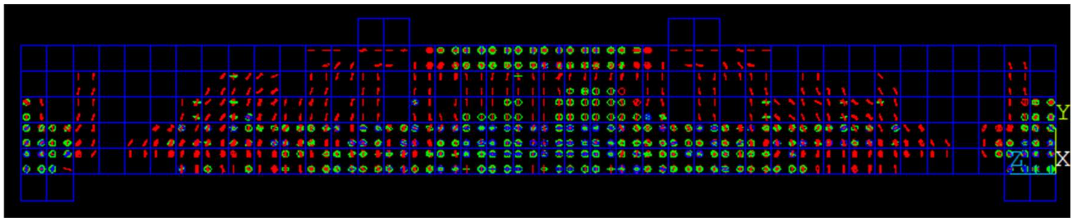

d) Numerical A0 block crack pattern

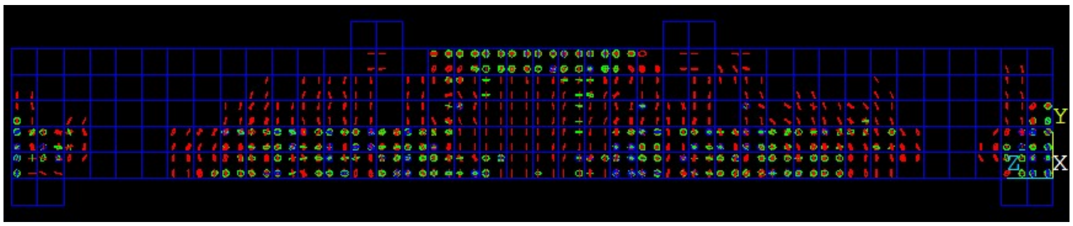

c) Numerical A7 beam cracking pattern

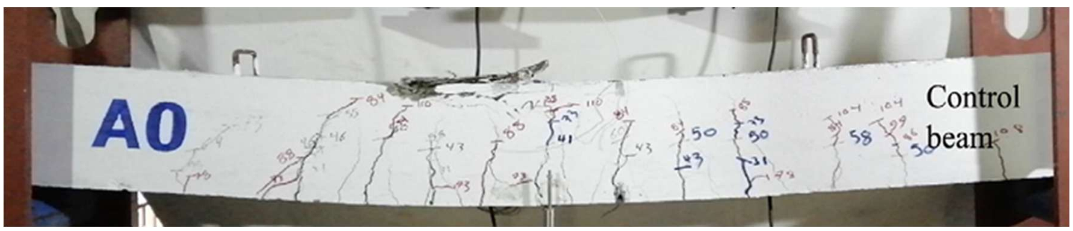

b) Experimental A0 block cracking pattern

a) Experimental A7 beam cracking pattern

Figure 4 Comparison of crack patterns from the experimental test and finite element analysis for A0 and A7 specimens.

Table 2 Comparison of experimental and numerical differences

Beam model	Pu (kN) Experiment	Pu (kN) Numeric	% Error Difference	δu (mm) Experiment	δu (mm) Numeric	% Error Difference
A0	118	125	5.95%	14.739	14.703	0.009%
A7	112	121.6	8.57%	12.0	11.878	1.02%

Conclusion

Based on the comparison between the experimental results and the numerical validation using ANSYS, the A0 beam exhibited a load discrepancy of 5.95% and a deflection discrepancy of 0.009%. Meanwhile, the A7 beam, which was exposed to elevated temperature, showed a load discrepancy of 8.57% and a deflection discrepancy of 1.02%, both of which remain within acceptable limits. Compared with the A0 beam, the load-carrying capacity of the A7 beam decreased by 5.08%, while its maximum deflection decreased by 18.58% after thermal exposure. Overall, these findings indicate that the numerical model can represent the experimental response with reasonable accuracy and may be used to reduce the number of test specimens and the costs associated with experimental testing.

References

Abdulrahman, A. S., & Kadir, M. R. A. (2022). Behavior and flexural strength of fire-damaged high-strength reinforced rectangular concrete beams after strengthening with CFRP laminates. *Ain Shams Engineering Journal, 13*(6), 101767. https://doi.org/10.1016/j.asej.2022.101767

ANSYS, Inc. (2025). *Basic analysis guide*. ANSYS.

Antonius, Purwanto, & Harprastanti, P. (2019). Experimental study of the flexural strength and ductility of post-burned steel fiber RC beams. *International Journal of Technology, 10*(2), 428–437. https://doi.org/10.14716/ijtech.v10i2.2097

Çalışkan, Ö., Aras, M., Yılmaz, T., & Anıl, Ö. (2025). Experimental and numerical investigation of low-velocity impact behavior and failure mode of shear-deficient RC beam strengthened with CFRP strips. *Structural Concrete, 26*(1), 856–878. https://doi.org/10.1002/suco.202301137

Cottrell, J. A., Ali, M., Tatari, A., & Martinson, D. B. (2021). An investigation into the influence of geometry on compressed earth building blocks using finite element analysis. *Construction and Building Materials, 273*, 121997. https://doi.org/10.1016/j.conbuildmat.2020.121997

Kodur, V. K. R., Naser, M. Z., & Kim, H. S. (2025). Fire performance of concrete structures incorporating FRP reinforcement: State-of-the-art and knowledge gaps. *Cement and Concrete Composites, 161*, 106074. https://doi.org/10.1016/j.cemconcomp.2025.106074

Krasnitskyi, P., & Lobodanov, M. (2024). Nonlinear modeling and analysis of damaged reinforced concrete beams using ANSYS and Lira-Sapr software packages. *Theory and Building Practice, 2024*(2), 39–49. https://doi.org/10.23939/jtbp2024.02.039

Kumar, P., & Kodur, V. K. R. (2023). Effect of fire-induced restraint forces on fire behavior of reinforced and prestressed concrete beams. *Engineering Structures, 275*, 115200. https://doi.org/10.1016/j.engstruct.2022.115200

Luu, X. B., Kim, S. K., & Kim, W. (2023). Investigation of load–displacement characteristics and crack behavior of RC beam based on nonlinear finite element analysis using concrete damage plasticity. *Applied Sciences, 13*(21), 11798. https://doi.org/10.3390/app132111798

Reynders, E. P. B., Godeau, J., Jovanović, B., van de Velde, M., Anastasopoulos, D., Lombaert, G., Caspeele, R., & Van Coile, R. (2025). Experimental analysis of the influence of moderate fire damage on the dynamic and incremental static behavior of reinforced concrete beams. *Engineering Structures, 323*, 119213. https://doi.org/10.1016/j.engstruct.2024.119213

Simwanda, L., Babafemi, A. J., Koker, N. de, & Viljoen, C. (2023). Bayesian calibration and reliability analysis of ultra-high-performance fibre reinforced concrete beams exposed to fire. *Structural Safety, 103*, 102352. https://doi.org/10.1016/j.strusafe.2023.102352

Song, Y., Fu, C., Liang, S., Li, D., Dang, L., Sun, C., & Kong, W. (2020). Residual shear capacity of reinforced concrete beams after fire exposure. *KSCE Journal of Civil Engineering, 24*(11), 3330–3341. https://doi.org/10.1007/s12205-020-1758-7

Suryanita, R., Maizir, H., Ismeddiyanto, Andriano, R., & Arditama, R. (2019). Experimental study and numerical analysis of flexural behaviour of post-fire reinforced concrete beam. *IOP Conference Series: Materials Science and Engineering, 615*(1), 012090. https://doi.org/10.1088/1757-899X/615/1/012090